Adsorption of Methanethiol on Stoichiometric and Defective TiO_2(110) Surfaces: A Combined Experimental and Theoretical Study

G. Liu, J. A. Rodriguez,* Z. Chang, and J. Hrbek

Department of Chemistry, Brookhaven National Laboratory, Upton, New York 11953

L. González

Instituto de Ciencia de Materiales, Universidad de Zaragoza, 50009, Zaragoza, Spain

Received: May 9, 2002; In Final Form: July 1, 2002

The interaction of CH_3SH with TiO_2(110) has been studied with a combination of synchrotron-based high-resolution photoemission, thermal desorption mass spectroscopy, and first-principles density functional slab calculations. On the Ti and O sites of a perfect TiO_2(110) substrate there is no dissociation of CH_3SH. The molecule bonds to Ti sites via its S lone pairs and desorbs at temperatures below 300 K. For CH_3SH chemisorbed on terraces of TiO_2(110), the desorption energies for molecular adsorption are ∼10−13 kcal/mol. The desorption energy for CH_3SH on defects is ∼18 kcal/mol. Photoemission results show that the active sites for the decomposition of CH_3SH are associated with oxygen vacancies ("$Ti^{\delta+}$" sites, $\delta \leq 3$). These defects induce occupied electronic states above the valence band of stoichiometric TiO_2 that bond well CH_3S, S, and C. Thus, the presence of O vacancies in the oxide surface allows the cleavage of the S−H bond in methanethiol and the deposition of CH_3S. The bond between CH_3S and O-vacancy sites is mainly covalent, but the bonding interactions are very strong and can induce the migration of O vacancies from the bulk to the surface of the oxide. In systems with a limited number of O vacancies, adsorbed CH_3S and H recombine and desorb as CH_3SH into gas phase. For surfaces with a large concentration of O vacancies and defects, the C−S bond in adsorbed CH_3S breaks in the 250−750 K temperature range with CH_3 or CH_4 desorbing into gas phase and leaving S and CH_x fragments on the surface. These results illustrate the important role played by O vacancies in the chemistry of a thiol over an oxide surface.

I. Introduction

Self-assembled monolayers (SAMs) of alkanethiols [R−SH, with R = $(CH_2)_nCH_3$] on metals and semiconductors are receiving a lot of attention due to possible technical applications in areas of biosensing, catalysis, tribology, and microelectronics.[1] In this respect, it is important to establish the nature of the interactions between the substrates and RS groups in the monolayer interface, including the identification of sites for molecular adsorption and dissociation, and the possible formation of lateral S−S bonds.[1−3] A complete understanding of these basic issues is necessary for tailoring the physical and chemical properties of SAM functional materials in a controlled manner.[1]

Methanethiol is the simplest anchor sulfur group of the alkanethiol systems that are used for preparing SAMs.[1] Many experimental[3−8] and theoretical[2,8−13] works have appeared examining the behavior of methanethiol on metal surfaces. Usually, the S−H bond breaks at very low temperatures (<150 K) producing adsorbed CH_3S groups.[3−7] The C−S bond in these groups usually dissociates between 250 and 450 K with S remaining on the surface, together with hydrocarbon fragments, while CH_4 and C_2H_6 desorb into gas phase.[3−8] An exception to these trends is found on Au(111),[3−7] where the dissociation of the molecule is limited. For oxide and semiconductor surfaces, only a few studies have been reported for the adsorption of methanethiol or alkanethiols in general.[14,15] The previous results show that alkanethiol SAMs can be formed on InP[16] and GaAs[17] semiconductor substrates. A recent study for the interaction of CH_3SH with polycrystalline ZnO shows that S−H bond cleavage occurs at 100 K.[14a] The formed CH_3S species are stable on the oxide surface up to ∼500 K, when they decompose producing S adatoms and products derived from the combustion (CO) or recombination of CH_3 (methane, ethane, acetylene, formaldehyde).[14a] No article has been published examining the interaction of CH_3SH with a well-defined oxide surface.

In this work, we investigate the chemistry of methanethiol on TiO_2(110) and TiO_{2-x}(110) using synchrotron based-photoemission, thermal desorption mass spectroscopy (TDS) and first-principle density-functional (DF) slab calculations. The rutile TiO_2(110) surface is one of the key model systems for metal oxide surfaces.[18,19] It has attracted a lot of attention due to the use of titania in catalysis and gas sensors.[20] In the chemical industry, titania is a catalyst used for the destruction of SO_2 in the Claus reaction, and a sorbent employed for trapping S-containing impurities (alkane thiols included) in oil-derived feedstocks.[14,21] Furthermore, systems of the RS−TiO_2 type are ideal for studying electron transfer between semiconductor particles and molecular wires,[15,16,22] and here a key point is the nature of the chemisorption bond (the "electrical junction" in practical terms). Previous studies have shown that the reactivity of the stoichiometric TiO_2(110) surface toward sulfur is low.[23−25] On the other hand, the presence of O vacancies leads to unexpected chemical transformation.[24,26] Therefore, we investigate defective surfaces to elucidate the role of oxygen vacancies in the surface chemistry of methanethiol on TiO_2-

* Corresponding author: Fax: 631-344-5815. E-mail: rodrigez@bnl.gov

10.1021/jp021155r CCC: $22.00 © 2002 American Chemical Society
Published on Web 08/24/2002

(110), i.e., molecular adsorption versus dissociation, and their effect on the properties of the RS−TiO_2 bond.

II. Experimental and Theoretical Methods

II.1. Sample Preparation, Photoemission, and TDS Experiments. The experimental work was carried out in two independent ultrahigh vacuum (UHV) chambers. The photoemission experiments were performed in a UHV chamber[27] at the U7A station in the National Synchrotron Light Source (NSLS) at Brookhaven National Laboratory. This chamber (with a base pressure of $\sim 5 \times 10^{-10}$ Torr) is fitted with a hemispherical electron energy analyzer with multichannel detection, optics for low-energy electron diffraction (LEED), a quadruple mass spectrometer (QMS), and a twin (Mg Kα and Al Kα) X-ray source. The combined energy resolution in the synchrotron experiments was 0.3−0.4 eV. The binding energy (BE) values were determined with respect to the Fermi energy. The TDS experiments were done in a second UHV chamber[3] (with a base pressure of $\sim 5 \times 10^{-10}$ Torr), which is equipped with a hemispherical electron energy analyzer with single channel detection, a twin X-ray source, and a residual gas analyzer (SRS−RGA). The residual gas analyzer was surrounded by a stainless steel jacket with a 10-mm aperture and a differential pumping system for TDS measurements. All the TDS spectra reported in section III were collected at a heating rate of 2 K/s. For the TDS measurements, the crystal was positioned 1−2 mm away from the aperture of the mass spectrometer jacket to prevent contributions of signals from surfaces other than the sample.

The TiO_2(110) single crystal was sandwiched between Ta plates that were spot-welded to two Ta heating legs of a manipulator.[23,24,27a] The sample could be cooled as low as 100 K by thermal contact with a liquid nitrogen reservoir and resistively heated to 1200 K. The temperature was monitored by a type C thermocouple inserted in a hole at the sample edge. Prior to each experiment the TiO_2(110) crystal was cleaned by repeated cycles of 1 keV Ne^+ ion bombardment followed by heating at 900 K until no impurities were detected by photoemission.[23,24] After this treatment the sample exhibited a sharp (1 × 1) LEED pattern.

High-purity (99+%) methanethiol (Aldrich) was further purified by several freeze−pump−thaw cycles with liquid nitrogen prior to dosing.[4b] The gas dosing was performed by backfilling the chamber through a leak valve, and all the reported exposures are based on the ion gauge reading in Langmuir units (1 L = 10^{-6} Torr·s). Mass spectrometry indicated that the reactants did not decompose significantly in the gas handling system or on the walls of the UHV system.

II.2. First-Principles Density Functional Calculation. We carried out self-consistent first-principles calculations within the Kohn−Sham density functional (DF) theory using the CASTEP (Cambridge Serial Total Energy Package) suite of programs.[28] CASTEP has an excellent track record in adsorption studies on TiO_2(110)[23,24,29−32] and other oxide surfaces.[28b,33−36] In this code, the wave functions of valence electrons are expanded in a plane wave basis set with k vectors within a specified energy cutoff E_{cut}. Tightly bound core electrons are represented by nonlocal ultrasoft pseudopotentials of the Vanderbilt type.[37] The valence s and p states of C, O, and S, plus the semicore (3s,3p) and valence (3d,4s,4p) states of Ti, are explicitly treated. Brillouin zone integration is approximated by a sum over special k points chosen using the Monkhorst−Pack scheme.[38] The exchange-correlation contribution to the total electronic energy is treated in a spin-polarized generalized gradient corrected (GGA) extension of the local density approximation (LDA).[39] In all of the calculations, the kinetic energy cutoff (E_{cut} = 400 eV) and the density of the Monkhorst−Pack k point mesh (a 8 × 4 × 1 grid for the smallest (1 × 1) surface unit cell, reduced to 4 × 4 × 1 or 4 × 2 × 1 grids for larger cells) were chosen high enough to ensure convergence of the computed structures and energetics. Since the DF calculations were performed at the GGA level, one can expect reasonable predictions for the bonding energies of the CH_3SH molecule on TiO_2(110) and TiO_{2-x}(110).[19,40,41] For the interaction of CO and NO with TiO_2-(110), DF-GGA calculations predict adsorption energies within an accuracy of 5 kcal/mol.[29,30,40b] An acceptable match is also found for the calculated and experimentally measured adsorption energies of S and S_2 on TiO_2(110).[23,24] In any case, in this work our main interest is in qualitative trends in the energetics, and not in absolute values. For each optimized structure, the partial charges on the atoms were estimated by projecting the occupied one-electron eigenstates onto a localized basis set with a subsequent Mulliken population analysis.[42,43] Mulliken charges have well-known limitations,[44] but experience has shown that they are nevertheless useful as a qualitative tool.[23,24,33,29,41−44]

Following previous studies,[24,27a,29,30] stoichiometric TiO_2(110) and surfaces with O vacancies were represented using four-layer slab models (Figure 1) embedded in a three-dimensionally periodic supercell.[24,28] A vacuum of 14 Å was placed on top of the slabs in order to ensure negligible interactions between periodic images normal to the surface.[28] The adsorbates (CH_3-SH, CH_3S, H) were set only on one side of the slabs, and their geometry and the geometry of the first two slab layers were relaxed during the DF calculations. This has proven to be a reliable approach to study the adsorption of CO, NO, NO_2, and S on TiO_2(110).[23,24,29,30] The DF calculations predicted accurate lattice constants for bulk TiO_2 and a structural geometry for the clean TiO_2(110) surface that was in agreement with several theoretical and experimental investigations.[23,29] In many situations it is unlikely that O vacancies in TiO_2 will assume a periodic array such as shown in Figure 1, but these models represent well electronic and chemical perturbations associated with the formation of O vacancies.[23,24,27a,29] The slab models are not appropriate to study the behavior of TiO_2(110) after heavy ion sputtering, which can lead to disordered surfaces with a large content of different types of defects.[18,20b,29]

III. Results and Discussion

III.1. Adsorption and Reaction of CH_3SH on TiO_2(110): TDS and XPS Results. Figure 2 shows typical TDS spectra for methanethiol adsorption on a well-ordered almost stoichiometric TiO_2(110) surface after a series of exposures at 100 K. Each spectrum in Figure 2 was obtained after an identical sputtering and annealing treatment, as described in section II.1. Previous studies show[45] that this treatment leads to a limited number of surface oxygen vacancies (<7%). The largest cracking fragment (m/e = 47 amu) of the methanethiol molecule was monitored, and CH_3SH was the only detectable desorption product observed in the temperature range between 100 and 900 K. No evidence for irreversible decomposition was found in TDS (i.e., no CH_4 and C_2H_6 formation or CH_3 evolution). It is well known that absolute coverages for adsorbates on TiO_2 surfaces are generally difficult to determine.[46] The integrated area of each TDS curve was used to determine the relative monolayer (ML) coverage reported in this work.[46] For 0.20 ML adsorption, only one desorption peak (T_{max} = 288 K) appears, labeled as α_1. The low intensity of this peak at saturation indicates that it is not associated with CH_3SH molecules

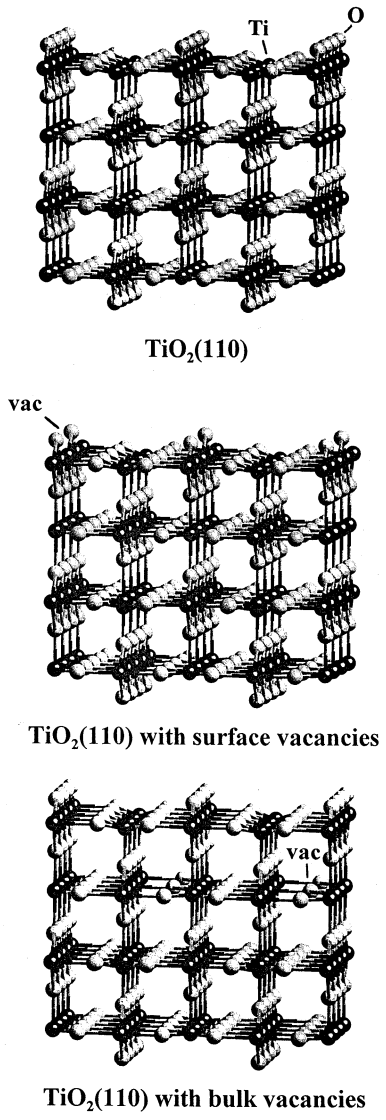

Figure 1. Four-layer slabs used to represent stoichiometric $TiO_2(110)$, top, and systems with O vacancies in the surface, center, or subsurface region, bottom.

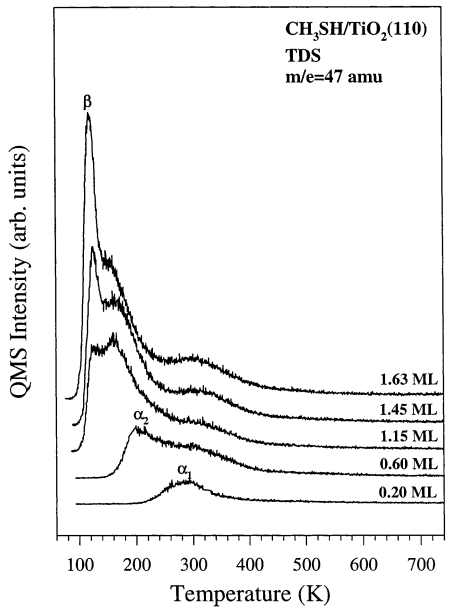

Figure 2. Thermal desorption spectra for methanethiol adsorption on a $TiO_2(110)$ surface at 100 K as a function of relative monolayer coverage. The ion signal (47 amu) was monitored. The heating rate (dT/dt) was 2 K/s.

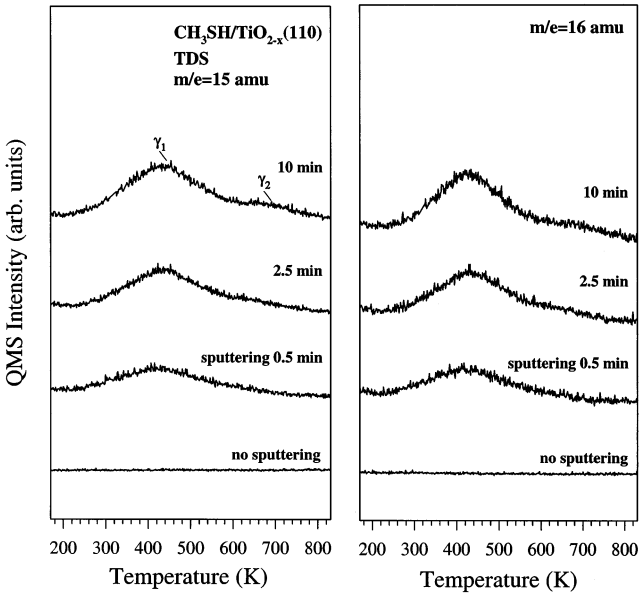

Figure 3. Thermal desorption spectra showing the evolution of CH_4 and CH_3 for CH_3SH adsorption on $TiO_{2-x}(110)$ surfaces with different $Ti^{\delta+}$ ($\delta \leq 3$) concentration. The methanethiol dose was 1.5 L in all cases, and the heating rate was 2 K/s.

interacting with terraces of $TiO_2(110)$. The α_1 peak probably originates from molecules bound on defect sites, either in a molecular adsorption or dissociated into CH_3S_a and H_a. The first hypothesis is more likely because no decomposition products for methanethiol were observed during these experiments. As the exposure increases, a second peak (α_2) with $T_{max} = 176$ K is seen at 0.60 ML. The α_2 state shifts (~80 K) to lower temperature with increasing exposure. Generally, the peak position shifting to lower temperatures with increasing exposures implies repulsive interactions between the adsorbed CH_3SH molecules.[3] The α_2 state is likely coming from CH_3SH adsorbed on terraces of $TiO_2(110)$, top of Figure 1. Finally, a relatively sharp peak (β) appears at 120 K with an exposure of 4.8 L (~1.63 ML in relative coverage units). The β peak grows without saturation and is assigned as the condensed multilayer desorption. The desorption temperature for the multilayer peak is consistent with values seen on metal surfaces.[3] The estimated desorption energies, according to the Redhead method,[47] assuming a first-order desorption kinetics and no intermolecular interactions with a preexponential factor of 10^{13} s^{-1}, are ~18 and 13−10 kcal/mol for the α_1 and α_2 states, respectively.

Henderson et al.[48a] studied the adsorption of CH_3OH on TiO_2-(110) and observed decomposition of the adsorbate only on surfaces rich with defects and O vacancies. O vacancies enhance the reactivity of $TiO_2(110)$ toward S_2.[23−25] We created O vacancies and defects on $TiO_2(110)$ by Ne^+ sputtering.[18,29] Heavy ion sputtering generates both lower oxidation cation states (i.e., $Ti^{\delta+}$ sites, $\delta \leq 3$) and extended structural defects (i.e., steps and/or kinks) by creating either bridging or in-plane oxygen vacancies.[29,48b] Images by scanning tunneling microscopy (STM) indicate that the surface becomes rough and disordered.[18b] Figure 3 shows thermal desorption spectra for methanethiol on sputtered $TiO_{2-x}(110)$ surfaces. The last set of data (10 min sputtering) corresponds to a disordered surface (no LEED pattern) that, according to Ti 2p photoemission data, contained ~55% of Ti^{4+}, 30% of Ti^{3+}, and 15% of Ti^{2+}.[29] The CH_3SH dose for each spectrum in Figure 3 is about 1.5 L. The

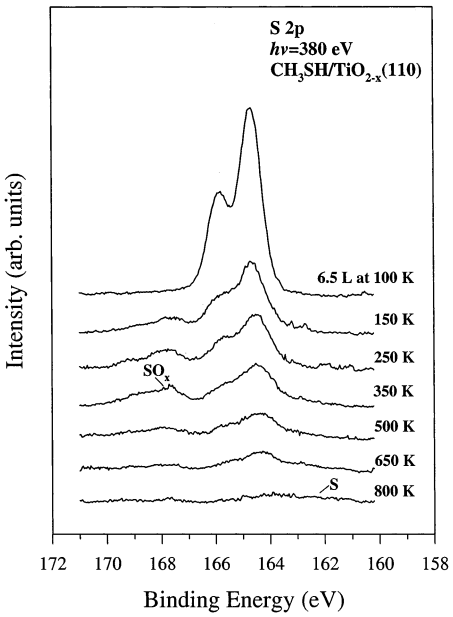

Figure 4. S 2p spectra ($h\nu = 380$ eV) for the adsorption of CH_3SH on a $TiO_{2-x}(110)$ surface slightly defective (~10% of Ti^{3+} centers). CH_3SH was dosed at 100 K, and the surface progressively annealed to the indicated temperatures.

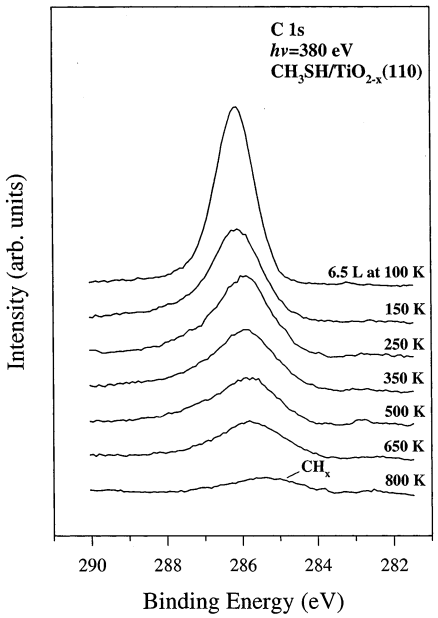

Figure 5. C 1s spectra ($h\nu = 380$ eV) for the adsorption of CH_3SH on the $TiO_{2-x}(110)$ surface of Figure 4. CH_3SH was dosed at 100 K, and the surface was progressively annealed to the indicated temperatures.

left panel of Figure 3 is for 15 amu and the right panel is for 16 amu. In addition to the parent CH_3SH TDS signal, methane (16 amu) and the methyl radical (15 amu) were observed to desorb at higher temperatures (T_{max}= 440 K, γ_1 state) after sputtering 0.5 min. An additional peak at 690 K (γ_2 state) developed beyond 2.5 min sputtering. No species other than methane, methyl radical (not from cracking pattern of CH_4[4b]), and methanethiol were found in TDS (i.e., no evolution of C_2H_6, C_2H_4, CH_2O, SO_2, or S_2). The desorption of methane or methyl radical indicates the irreversible decomposition of CH_3SH on the defective $TiO_{2-x}(110)$ surface. It is possible that the CH_4 formation is partly due to H-atom abstraction from the mass spectrometer shield as a result of collisions of methyl radical with the walls.[49] The CH_3SH parent ion signal was still seen, even for the 10 min sputtering (not shown).

Photoemission was used to study the interaction of CH_3SH and $TiO_{2-x}(110)$ surfaces with a low or medium concentration of O vacancies. Figure 4 displays the changes in S 2p core level photoemission spectra for the dosing of 6.5 L of CH_3SH to a $TiO_{2-x}(110)$ surface slightly defective (~10% concentration of Ti^{3+} according to Ti 2p spectra[27a]) at 100 K, and sequentially annealing to high temperatures. TDS results showed that multilayer CH_3SH should be formed upon a 6.5 L exposure at 100 K. Only one dominant doublet between 166 and 164 eV is seen at 100 K, with the S $2p_{3/2}$ BE value at 164.7 eV, similar to values reported previously for CH_3SH multilayer.[50] Heating to 150 K causes a rapid decrease in the intensity of the multilayer features (see TDS data in Figure 2) and the appearance of at least two types of sulfur chemisorbed species. The dominant one is CH_3S or CH_3SH (we were unable to distinguish these compounds in photoemission), and the other is probably related to the formation of a small amount of SO_x[23] by decomposition of CH_3SH on highly reactive sites. The intensity of the S 2p features reduces by ~40% upon heating from 150 to 350 K. Heating to 650 K reduces again the S 2p intensity, and the SO_x features disappear. How the small amount of SO_x formed decomposes is not clear, since we did not detect significant signals for S, S_2, or SO_2 in TDS. In Figure 4, a trace of sulfur is still seen at ~162 eV after heating to 800 K, probably atomic sulfur.[23,24]

The corresponding C 1s core level spectra for the experiments in Figure 4 are shown in Figure 5. For the condensed multilayer at 100 K, the C 1s BE is ~ 286 eV, which is in good agreement with the C 1s values seen for multilayer CH_3SH on metal surfaces.[3] Heating to 150 K removes the CH_3SH multilayer (see Figure 2). From 150 to 800 K, there is continuous decrease of the C 1s signal that was accompanied by desorption of CH_3SH, CH_3, and CH_4 according to TDS. By 800 K, the C 1s signal is still seen, probably due to CH_x species[50] produced by the extensive decomposition of some methanethiol molecules on the defect sites.

Figures 6−8 display photoemission spectra (Ti 2p, S 2p, and C 1s core levels) for the adsorption of CH_3SH on a $TiO_{2-x}(110)$ surface with a larger amount of defect sites. The surface was generated by ion sputtering, and the Ti 2p spectra obtained before the adsorption of CH_3SH (Figure 6) showed a concentration of ~20% of $Ti^{\delta+}$ ($\delta = 2$ or 3) sites after curve fitting.[29] The adsorption of a CH_3SH multilayer at 100 K produces a large attenuation in the Ti 2p signal. The intensity is recovered after heating to 800 K and desorbing most of the overlayer. At the end, a small amount of S and CH_x remains on the surface (see below) and probably induces a change in band bending[20a,51] with a shift in the Ti 2p positions.

Figure 7 shows the corresponding S 2p core level spectra for CH_3SH adsorption at 100 K followed by heating to the indicated temperatures. The spectrum at 100 K is a typical one for a physisorbed multilayer of CH_3SH with the S $2p_{3/2}$ peak position at 164.7 eV. By 150 K (after desorbing the CH_3SH multilayer), an additional feature is present around 162.0 eV, which probably arises from atomic sulfur species.[23,24] The results in Figure 7 indicate that on the defect-rich $TiO_2(110)$ surface there is substantial decomposition of CH_3SH at very low temperature (≤150 K) with the sulfur going to O centers (SO_x formation)[23,27a] or Ti centers (S deposition).[23,24] Nevertheless, the dominant S 2p features still appear between 166.5 and 163.5 eV and correspond to adsorbed CH_3SH or CH_3S. Heating from 150 to 800 K leads to a continuous decrease in the signal for

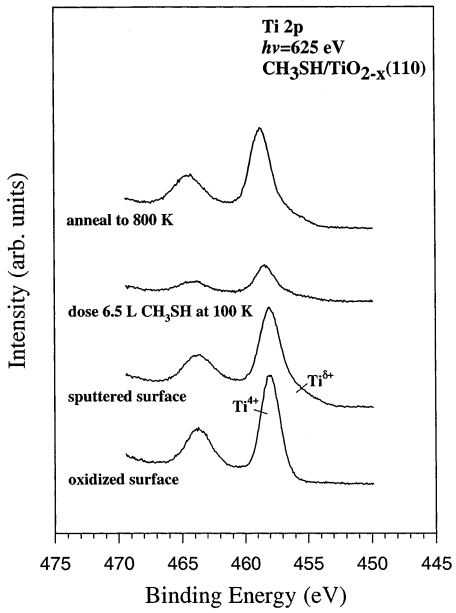

Figure 6. Ti 2p spectra taken before and after dosing of methanethiol to a TiO_{2-x}(110) surface with a substantial amount of $Ti^{\delta+}$ ($\delta \leq 3$) sites (~20%). The spectra were obtained using a photon energy of 625 eV.

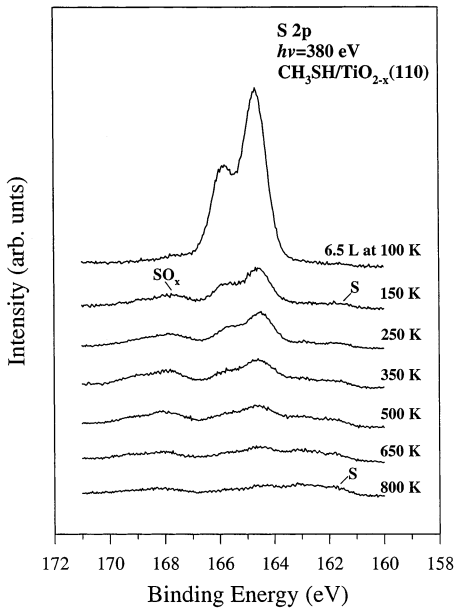

Figure 7. S 2p spectra ($h\nu = 380$ eV) for the adsorption of CH_3SH on the TiO_{2-x}(110) surface of Figure 6. CH_3SH was dosed at 100 K, and the surface progressively annealed to the indicated temperatures.

the SO_x and CH_3SH/CH_3S species, while there is a slight increase in the signal for atomic S.

Figure 8 displays the C 1s core level data for the experiments in Figures 6 and 7. The C 1s multilayer feature appears at ~286 eV. In agreement with Figure 7, a weak feature is seen around 283 eV at 100 K, indicating the extensive decomposition of parent CH_3SH molecules, probably to form carbonaceous species on the defects.[50] Annealing to 150 K drastically reduces the multilayer intensity. The intensity of the C 1s signal at ~283 eV gradually increases up to 700 K, whereas the C 1s feature located as ~286 eV decreases. By heating to 650 K, the intensities of these two C 1s features are comparable, suggesting a partial transformation of CH_3S or CH_3SH to CH_x.[50]

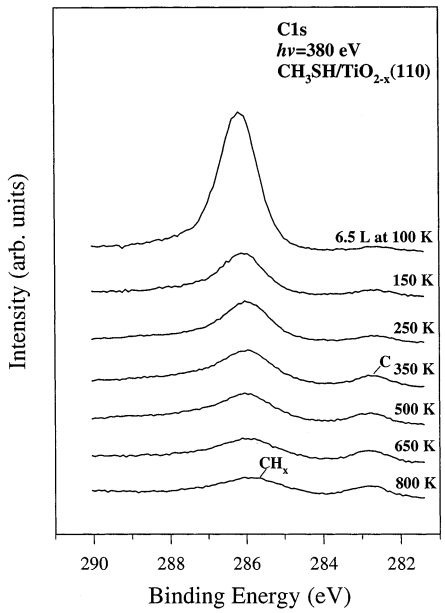

Figure 8. C 1s spectra ($h\nu = 380$ eV) for the adsorption of CH_3SH on the TiO_{2-x}(110) surface of Figure 6. CH_3SH was dosed at 100 K, and the surface was progressively annealed to the indicated temperatures.

In summary, the results of the present work show the importance of O vacancies and defects on the surface chemistry of a thiol/oxide system. Methanethiol interacts weakly with a well-defined perfect oxide, but upon the introduction of O vacancies the oxide surface can become as reactive as a metal.[3−8] The following mechanism for methanethiol adsorption and decomposition on TiO_2(110) is proposed:

$$CH_3SH_g \rightarrow CH_3SH_a \quad (1)$$

$$CH_3SH_g \rightarrow CH_3S_a + H_a \quad (2)$$

The initial adsorption of methanethiol can be either molecular on terraces [reaction 1] or dissociative to generate thiolates [reaction 2] on defect sites. Reaction 2 could be reversible during TDS to form methanethiol by recombination of CH_3S_a and H_a if the concentration of O vacancies and defects is very low. To replace the oxygen vacancies, the C−S bond must be broken and the sulfur atoms and CH_x fragments could be incorporated at the vacancy sites. The adsorbed CH_3S_a could further react with surface oxygen to form SO_x during heating.

$$CH_3S_a + xO_s \rightarrow CH_{3a} + SO_x \quad (3)$$

The decomposition of adsorbed CH_3S produces gaseous CH_3.

$$CH_3S_a \rightarrow CH_{3g} + S_a \quad (4)$$

The methyl radicals can react with adsorbed H_a to form CH_4, or they can decompose further to adsorbed C and CH_x.

$$CH_{3a} + H_a \rightarrow CH_{4g} \quad (5)$$

$$nCH_{3a} \rightarrow mCH_{4g} + (n-m)CH_{xa} \quad (n > 1) \quad (6)$$

It has been reported that on polycrystalline ZnO films[14a] and partially hydroxylated powders of TiO_2,[14b] the reactivity of methanethiol is very significant. At 100 K, methanethiol adsorption undergoes an acid−base reaction to form a thiolate species.[14a] Above 500 K, C−S bond cleavage occurs to produce carbon monoxide, methane, formaldehyde, ethane, and a mixture

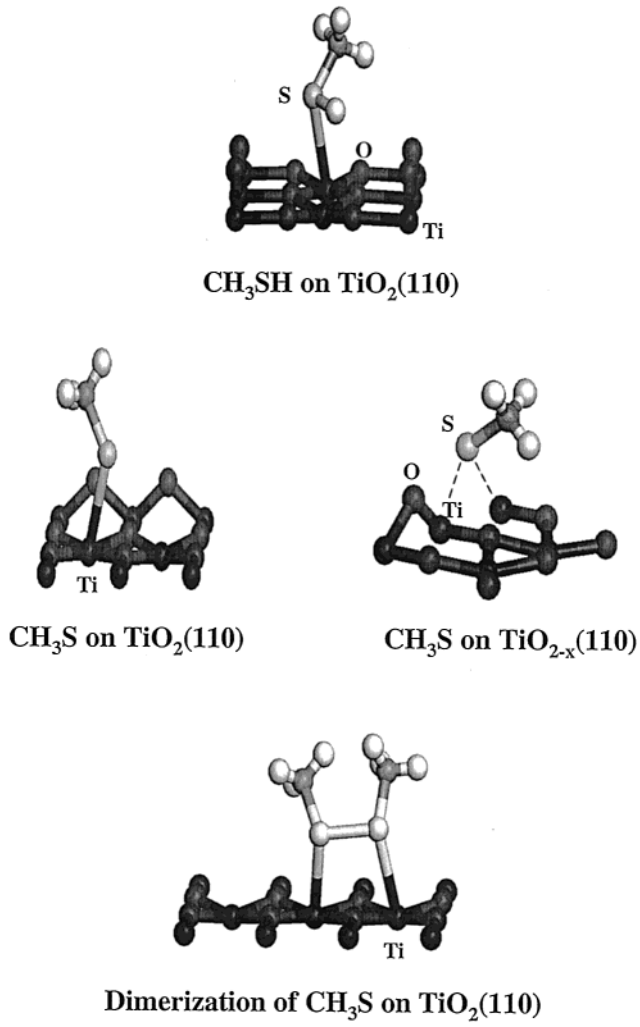

Figure 9. Calculated adsorption geometries for CH_3SH on Ti rows of TiO_2(110), top; CH_3S on Ti rows and O vacancies of TiO_2(110), center left and right, respectively; high coverage of CH_3S ($\theta = 0.66$ ML) on Ti rows of TiO_2(110), bottom.

of ethylene and acetylene, with substantial amounts of atomic sulfur remaining on the surface.[14a] Methane is the main product of the reaction of CH_3SH with partially hydroxylated powders of TiO_2.[14b] The differences in methanethiol reactivity between single-crystal TiO_2(110) and the polycrystalline oxides are partly due to the surface structures. For polycrystalline ZnO and TiO_2 there are a lot of surface imperfections that facilitate the initial cleavage of the S−H bond at low temperature,[14] but the lack of O vacancies makes difficult the subsequent breaking of the C−S bond (not at < 150 K as seen in Figures 7 and 8). The chemical reactivity of stoichiometric TiO_2(110) is rather low,[19,20b,23,48] but O vacancies facilitate the extensive decomposition of CH_3OH,[48a] SO_2,[27] and hydrocarbons.[20b] The low reactivity of TiO_2(110) is partly due to its surface structure (top of Figure 1), which exposes the out-of-plane bridging oxygen anions and pentacoordinated Ti cations.[20c] In the following section we will examine in more detail the bonding of CH_3SH to TiO_2(110) and the complex interactions between the adsorbate and O vacancies.

III.2. Bonding of CH_3SH and CH_3S to TiO_2(110). In the first part of this section, we will study the bonding of CH_3SH to a perfect TiO_2(110) surface using first-principles density functional calculations and the four-layer slab model shown at the top of Figure 1. Methanethiol can interact with the Ti and O centers via S or H. The top of Figure 9 displays the most

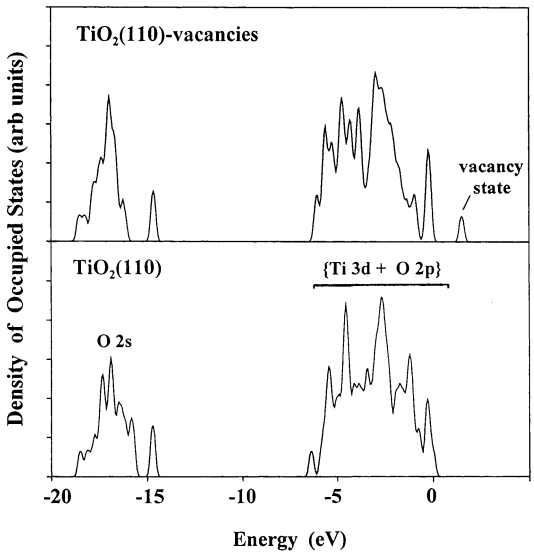

Figure 10. Calculated density-of-states (DOS) for the occupied bands of a perfect TiO_2(110) slab (bottom of figure) and a TiO_{2-x}(110) slab with O vacancies on the surface (top of figure).

stable coordination found for the molecule at coverages of 0.25 ML, p(2 × 2) array, and 0.50 ML, p(2 × 1) array. The binding of CH_3SH is essentially a consequence of Ti−S interactions that involve the occupied S lone pairs of the molecule and empty 3d and 4s, p orbitals of titanium. The Ti−S bond length varies from 3.06 ($\theta = 0.25$ ML) to 3.18 Å ($\theta = 0.50$ ML), while the adsorption energy drops from 15 to 11 kcal/mol in the examined coverage range. These values are very different from those found in our previous calculations for atomic sulfur on the same surface (Ti−S = 2.41 and 2.46 Å; AE = 67 and 60 kcal/mol),[24] but are comparable to those obtained in DF-GGA calculations for the bonding of H_2S to a titania cluster (Ti−S = 3.10 Å; AE = 7 kcal/mol)[52] or adsorption energies (13−10 kcal/mol) estimated from our TDS experiments for CH_3SH/TiO_2(110).

On the stoichiometric TiO_2(110) surface, there was a small charge transfer (∼0.12e) from the CH_3SH adsorbate to the oxide substrate and negligible changes in the C−S (1.80 Å) and S−H (1.35 Å) bond distances with respect to free methanethiol. Our calculations indicate that the dissociation of adsorbed CH_3SH into CH_3S (on Ti centers) and H (on O centers) is an uphill process with the associated ΔE varying from +4 to +7 kcal/mol, depending on coverage (0.25 and 0.50 ML of CH_3SH) and adsorption sites. This agrees with the lack of significant dissociation seen in the experiments of section III.1 on nearly perfect TiO_2(110) surfaces.

Figure 10 shows the calculated density-of-states for the occupied bands of a TiO_{2-x}(110) slab with O vacancies on the surface (center of Figure 1) and a perfect TiO_2(110) slab (top of Figure 1). The valence band in TiO_2(110) contains states with O 2p and Ti 3d character.[19,24,53] The introduction of O vacancies in the TiO_2(110) surface generates a new occupied state that appears ∼1.6 eV above the top of the {O 2p + Ti 3d} band and has Ti 3d character. This state has been observed in experiments of valence photoemission[18] and is ideal for interacting with the decomposition products of methanethiol (CH_3S, S), which are species with a high electronegativity.[54,55] Thus, for the adsorption energy of CH_3S we calculate an increase close to 20 kcal/mol when going from pentacoordinated Ti in TiO_2(110) to Ti sites near O vacancies in TiO_{2-x}(110), center of Figure 9. Furthermore, a dissociation reaction of the type shown in Figure 11 ($CH_3SH_a \rightarrow CH_3S_a + H_a$) is substantially exothermic ($\Delta E = -17$ kcal/mol). These results highlight the

Figure 11. Calculated (DF-GGA) energy change for the dissociation of adsorbed CH_3SH ($\theta = 0.25$ ML) on a $TiO_{2-x}(110)$ surface. Initially, CH_3SH is located above a Ti row and then dissociates with CH_3S covering an O vacancy and H above a bridging oxygen.

important role played by O vacancies in the chemistry of a thiol on titania. Our calculations indicate that, in this respect, it is not only the existence of O vacancies at the surface that is important. Even if these defects are present in the subsurface region, they still can affect the chemical behavior of the oxide by migrating to the surface for interactions with the adsorbate.

Using the two slab models shown at the center and bottom of Figure 1, one can compare the stability of O vacancies in the surface and subsurface regions of $TiO_2(110)$.[24,29] DF calculations predict a small difference in stability (~3 kcal/mol) that favors the structure with subsurface vacancies.[24,27a] Thus, at temperatures ≤300 K, bulk and surface vacancies should coexist in a titania sample, and this is what is observed experimentally.[18,24,26] When CH_3SH is present on the surface, the migration of O vacancies from the subsurface region to the surface (see Figure 12) becomes a significantly exothermic process ($\Delta E = -15$ kcal/mol). One has a complex situation in which the O vacancies determine the chemistry of the adsorbate, and at the same time the adsorbate could probably affect the rate of exchange of these defects between the bulk and surface of the oxide.

The DF calculations indicate that isolated O-vacancy sites are not enough to induce the full decomposition of the CH_3SH molecule. Once S−H bond breaking has occurred and CH_3S is covering the O vacancy, the decomposition reaction should stop, because C−S bond breaking with CH_3 going to normal Ti and O sites is a very endothermic process ($\Delta E > +10$ kcal/mol). Two close O vacancies are necessary to induce sequential S−H and C−S bond cleavage. This is consistent with the photoemission and TDS studies described in the previous section, which show full decomposition of CH_3SH on the oxide surface only after substantial ion sputtering.

Systems of the RS−TiO_2 type are ideal for studying electron transfer between semiconductor surfaces and molecular wires,[12,16,22] and here key issues are the possible formation of lateral S−S bonds[1−3] and the nature of the chemisorption bond (the "electrical junction" in practical terms).[16,22] In previous studies for $S/TiO_2(110)$,[23,24] we found evidence for S−S bonding on the surface when the adsorbate coverage was larger than 0.5 ML. Under these conditions, the oxide substrate was not able to respond in an effective way to the large number of adsorbed species, and S−S bonds were formed to compensate for the relatively weak Ti−S bonds. A similar phenomenon is observed for the deposition of sulfur on several metals.[8,56,57] We investigated if something similar could occur for CH_3S on titania.

CH_3S groups adsorbed above O vacancies (center of Figure 9) interact with TiO_2 too strongly to allow CH_3S-SCH_3 bonding. On the other hand, the bonding interactions of CH_3S with atoms in the Ti rows of $TiO_2(110)$ are not very strong and could permit dimerization of the adsorbate. For 0.25 ML of CH_3S on the Ti rows, we found that a p(2 × 2) array of isolated CH_3S groups was clearly the most stable configuration for the

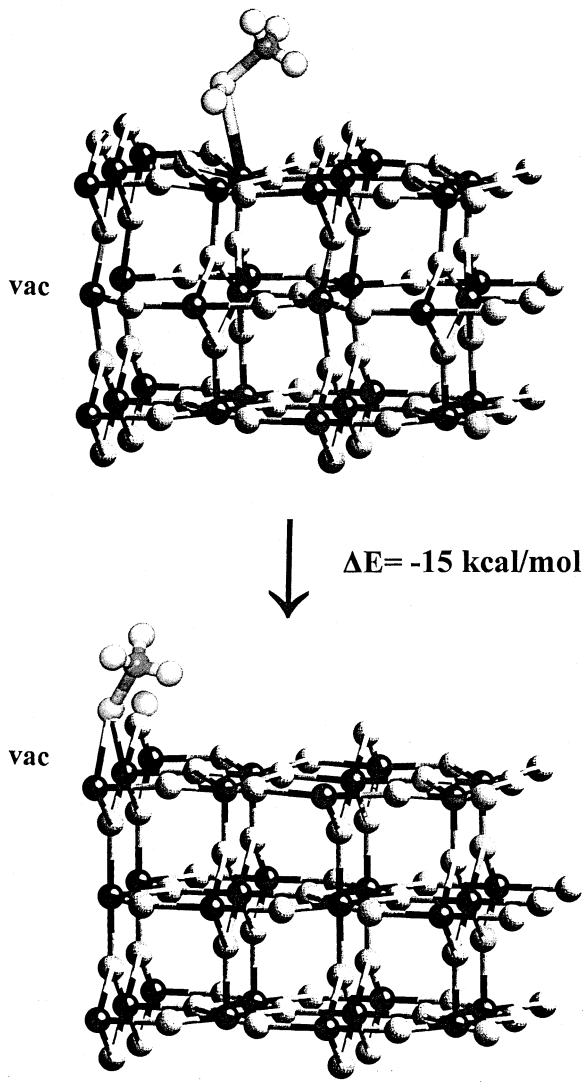

Figure 12. Calculated (DF-GGA) energy change for the CH_3SH-induced migration of O vacancies from the bulk to the surface of $TiO_{2-x}(110)$. Initially, the O vacancies are in the subsurface region and CH_3SH is adsorbed on the Ti rows. In the final state, the O vacancies have moved to the surface and are capped by CH_3S with H bonded to bridging oxygen.

overlayer. However, evidence for significant S−S interactions was observed at high coverages of CH_3S in our DF calculations. At the bottom of Figure 9, the optimal geometry obtained for 0.66 ML of CH_3S on the Ti rows of $TiO_2(110)$ is shown. The calculated sulfur-to-sulfur separation (2.09 Å) is not very different from that found experimentally for free CH_3SSCH_3 (2.04 Å[58]). Experimentally, the main problem here is the generation of such a large amount of CH_3S on the oxide surface from the decomposition of CH_3SH on the Ti rows.

In the junction of a semiconductor and a molecular wire, the overall conductivity of the system is affected by the degree of mixing or hybridization between the semiconductor bands and the molecule orbitals.[15−17] An important point is the distribution of charge in the molecule-semiconductor bond. Since CH_3S has a relatively large electron affinity (1.88 eV[55]) and titanium dioxide is far from being fully ionic,[24,29,53] the CH_3S-TiO_2 bond could involve a substantial charge transfer. Charges derived from a Mulliken population analysis[42,43] indicate that this bond is essentially covalent. On the Ti rows of a perfect $TiO_2(110)$ surface, the calculated negative charge on adsorbed CH_3S varied from −0.09 e (0.25 ML), to −0.06 e (0.50 ML), and −0.02 e

(0.66 ML). CH_3S molecules bonded to O-vacancy sites of TiO_{2-x}(110) also did not have large negative charges (−0.23 e at 0.25 ML; −0.19 e at 0.50 ML). In titania the excess of electronic charge produced by the creation of O vacancies is not highly localized on the vacancy sites (as in the case of MgO[59]) but distributed among the neighboring cations.[24,60] This charge delocalization seems to affect the bonding of adsorbates, and species such as CH_3S, S,[24] and SO_2[27a] do not receive a large charge transfer from the O-vacancy sites of TiO_{2-x}(110).

IV. Summary and Conclusions

High-resolution photoemission, TDS, and DF slab calculations were used to carry out the first systematic study of the interaction of CH_3SH with a well-defined oxide surface. On the Ti and O sites of a perfect TiO_2(110) substrate there is no dissociation of CH_3SH. The molecule bonds to Ti sites via its S lone pairs and desorbs at temperatures below 300 K. TDS experiments show molecular desorption peaks in the range 206−160 K (corresponding to desorption energies of ∼13−10 kcal/mol) that can be attributed to CH_3SH chemisorbed on terraces of TiO_2(110). From defect sites, methanethiol desorbs at relatively high temperature, ∼288 K, with a desorption energy of ∼18 kcal/mol.

The presence of O vacancies in the oxide surface produces electronic states that facilitate the cleavage of the S−H bond and the deposition of CH_3S. The bond between CH_3S and O-vacancy sites is mainly covalent, but the bonding interactions are very strong and can induce the migration of O vacancies from the bulk to the surface of the oxide. In systems with a limited number of O vacancies, adsorbed CH_3S and H can recombine and desorb as CH_3SH into gas phase. For surfaces with a large concentration of O vacancies and defects, there is extensive decomposition of CH_3SH at 100 K, producing a mixture of SO_x, CH_x, S, and CH_3S on the oxide. The C−S bond in adsorbed CH_3S breaks in the 250−750 K temperature range, with CH_3 or CH_4 desorbing into gas phase and leaving S and CH_x fragments on the surface. These results illustrate the important role played by O vacancies in the chemistry of a thiol over an oxide surface.

Acknowledgment. The authors at BNL thank the financial support of the U.S. Department of Energy (DOE), Division of Chemical Sciences under contract DE-AC02-98CH10886. The NSLS is supported by the Division of Materials and Chemical Sciences of DOE. L.G. is grateful to ENRI and the European Union for research grants that made possible part of this work.

References and Notes

(1) (a) Schreiber, F. *Prog. Surf. Sci.* **2000**, *65*, 151, and references therein. (b) Ulman, A. *Self-Assembled Monolayers of Thiols*; Academic Press: New York, 1998.

(2) Gottschalck, J.; Hammer, B. *J. Chem. Phys.* **2002**, *116*, 784, and references therein.

(3) Liu, G.; Rodriguez, J. A.; Dvorak, J.; Hrbek, J.; Jirsak, T. *Surf. Sci.* **2002**, *505*, 295, and references therein.

(4) (a) Friend, C. M.; Chen, D. A. *Polyhedron* **1997**, *16*, 3165. (b) Batteas, J. D.; Rufael, T. S.; Friend, C. M. *Langmuir* **1999**, *15*, 2391.

(5) Rufael, T. S.; Huntley, D. R.; Mullins, D. R.; Gland, J. L. *J. Phys. Chem.* **1995**, *99*, 11472.

(6) Cheng, L.; Bocarsly, A. B.; Bernasek, S. L. *Langmuir* **1996**, *12*, 392.

(7) Nuzzo, R. G.; Zegarski, B. R.; Dubois, L. H. *J. Am. Chem. Soc.* **1987**, *109*, 733.

(8) Rodriguez, J. A.; Hrbek, J. *Acc. Chem. Res.* **1999**, *32*, 719.

(9) Sellers, H.; Ulman, A.; Shnidman, Y. Eilers, J. E. *J. Am. Chem. Soc.* **1993**, *115*, 9389.

(10) Vargas, M. C.; Giannozzi, P.; Selloni, A.; Scoles, G. *J. Phys. Chem. B* **2001**, *105*, 9509.

(11) Grönbeck, H.; Curioni, A.; Andreoni, W. *J. Am. Chem. Soc.* **2000**, *122*, 3839.

(12) Hayashi, T.; Morikawa, Y.; Nozoye, H. *J. Chem. Phys.* **2001**, *114*, 7615.

(13) Häkkinen, H.; Barnett, R. N.; Landman, U. *Phys. Rev. Lett.* **1999**, *82*, 3264.

(14) (a) Dvorak, J.; Jirsak, T.; Rodriguez, J. A. *Surf. Sci.* **2001**, *479*, 155. (b) Beck, D. D.; White, J. M.; Ratcliffe, C. T. *J. Phys. Chem.* **1986**, *90*, 3137.

(15) Gu, Y.; Waldeck, D. H. *J. Phys. Chem. B* **1998**, *102*, 9015.

(16) (a) Yamamoto, H.; Butera, R. A.; Gu, Y.; Waldeck, D. H. *Langmuir* **1999**, *15*, 8640. (b) Gu, Y.; Kumar, K.; Lin, Z.; Read, I.; Zimmt, M. B.; Waldeck, D. H. *J. Photochem. Photobiol. A: Chem.* **1997**, *105*, 189. (c) Gu, Y.; Lin, Z.; Butera, R. A.; Smentkowski, V. S.; Waldeck, D. H. *Langmuir* **1995**, *11*, 1849. (d) Zerulla, D.; Mayer, D.; Hallmeier, K. H.; Chassé, T. *Chem. Phys. Lett.* **1999**, *311*, 8.

(17) (a) Sheen, C. W.; Shi, J.-X.; Mårtensson, J.; Parikh, A. N.; Allara, D. L. *J. Am. Chem. Soc.* **1992**, *114*, 1514. (b) Nakagawa, O. S.; Ashok, S.; Sheen, C. W.; Mårtensson, J.; Allara, D. L. *Jpn. J. Appl. Phys.* **1991**, *30*, 3759.

(18) (a) Henrich, V. E.; Cox, P. A. *The Surface Science of Metal Oxides*; Cambridge University Press: Cambridge, 1994. (b) Szabo, A.; Engel, T. *Surf. Sci.* **1995**, *329*, 241.

(19) Rodriguez, J. A. *Theor. Chem. Acc.* **2002**, *107*, 117.

(20) (a) Linsebigler, A. L.; Lu, G.; Yates, J. T., Jr. *Chem. Rev.* **1995**, *95*, 735. (b) Barteau, M. A. *Chem. Rev.* **1996**, *96*, 1413. (c) Idriss, H.; Barteau, M. A. *Adv. Catal.* **2000**, *45*, 261.

(21) (a) Piéplu, A.; Saur, O.; Lavalley, J. C.; Legendre, O.; Nédez, C. *Catal. Rev.-Sci. Eng.* **1998**, *40*, 409. (b) Satterfield, C. N. Heterogeneous Catalysis in Practice; McGraw-Hill: New York, 1981.

(22) González, C., personal communication.

(23) Rodriguez, J. A.; Hrbek, J.; Dvorak, J.; Jirsak, T.; Maiti, A. *Chem. Phys. Lett.* **2001**, *336*, 377.

(24) Rodriguez, J. A.; Hrbek, J.; Chang, Z.; Dvorak, J.; Jirsak, T.; Maiti, A. *Phys. Rev. B* **2002**, *65*, 235414.

(25) Hebenstreit, E. L. D.; Hebenstreit, W.; Diebold, U. *Surf. Sci.* **2000**, *461*, 87. Hebenstreit, E. L. D.; Hebenstreit, W.; Diebold, U. *Surf. Sci.* **2001**, *470*, 347.

(26) Hebenstreit, E. L. D.; Hebenstreit, W.; Geisler, H.; Ventrice, C. A.; Sprunger, P. T.; Diebold, U. *Surf. Sci.* **2001**, *486*, L467.

(27) (a) Rodriguez, J. A.; Liu, G.; Jirsak, T.; Hrbek, J.; Chang, Z.; Dvorak, J.; Maiti, A. *J. Am. Chem. Soc.* **2002**, *124*, 5242. (b) Liu, G.; Rodriguez, J. A.; Hrbek, J.; Dvorak, J.; Peden, C. H. F. *J. Phys. Chem. B* **2001**, *105*, 7762.

(28) (a) Payne, M. C.; Allan, D. C.; Arias, T. A.; Johannopoulus, J. D. *Rev. Mod. Phys.* **1992**, *64*, 1045. (b) Milman, V.; Winkler, B.; White, J. A.; Pickard, C. J.; Payne, M. C.; Akhmatskaya, E. V.; Nobes, R. H. *Int. J. Quantum Chem.* **2000**, *77*, 895.

(29) Rodriguez, J. A.; Jirsak, T.; Liu, G.; Hrbek, J.; Dvorak, J.; Maiti, A. *J. Am. Chem. Soc.* **2001**, *123*, 9597.

(30) (a) Sorescu, D. C.; Rusu, C. N.; Yates, J. T., Jr. *J. Phys. Chem. B* **2000**, *104*, 4408. (b) Sorescu, D. C.; Yates, J. T., Jr. *J. Phys. Chem. B* **1998**, *102*, 4556. (c) Casarin, M.; Maccato, C.; Vittadini, A. *J. Phys. Chem. B* **1998**, *102*, 10752.

(31) Dawson, I.; Bristowe, P. D.; Lee, M. H.; Payne, M. C.; Segall, M. D.; White, J. *Phys. Rev. B* **1996**, *54*, 13727.

(32) Lindan, P. J. D.; Harrison, N. M.; Holender, J. M.; Gillan, M. J. *Chem. Phys. Lett.* **1996**, *261*, 246.

(33) Rodriguez, J. A.; Pérez, M.; Jirsak, T.; González, L.; Maiti, A.; Larese, J. Z. *J. Phys. Chem. B* **2001**, *105*, 5497.

(34) Rodriguez, J. A.; Maiti, A. *J. Phys. Chem. B* **2000**, *104*, 3630.

(35) Refson, K.; Wogelius, R. A.; Fraser, D. G.; Payne, M. C.; Lee, M. H.; Milman, V. *Phys. Rev. B* **1995**, *52*, 10823.

(36) (a) Rodriguez, J. A.; Jirsak, T.; Pérez, M.; Chaturvedi, S.; Kuhn, M.; González, L.; Maiti, A. *J. Am. Chem. Soc.* **2000**, *122*, 12362. (b) Rodriguez, J. A.; Pérez, M.; Jirsak, T.; González, L.; Maiti, A. *Surf. Sci.* **2001**, *477*, L279.

(37) Vanderbilt, D. *Phys. Rev. B* **1990**, *41*, 7892.

(38) Monkhorst, H. J.; Pack, J. D. *Phys. Rev. B* **1976**, *13*, 5188.

(39) White, J. A.; Bird, D. M. *Phys. Rev. B* **1994**, *50*, 4954.

(40) (a) van Santen, R. A.; Neurock, M. *Catal. Rev.-Sci. Eng.* **1995**, *37*, 557. (b) Ziegler, T. *Chem. Rev.* **1991**, *91*, 651.

(41) Rodriguez, J. A.; Jirsak, T.; Pérez, M.; González, L.; Maiti, A. *J. Chem. Phys.* **2001**, *114*, 4186.

(42) Segall, M. D.; Pickard, C. J.; Shah, R.; Payne, M. C. *Phys. Rev. B* **1996**, *54*, 16317.

(43) Segall, M. D.; Pickard, C. J.; Shah, R.; Payne, M. C. *Mol. Phys.* **1996**, *89*, 571.

(44) (a) Szabo, A.; Ostlund, N. S. *Modern Quantum Chemistry*; McGraw-Hill: New York, 1989. (b) Wiberg, K. B.; Rablen, P. R. *J. Comput. Chem.* **1993**, *14*, 1504.

(45) Hrbek, J.; Rodriguez, J. A.; Dvorak, J.; Jirsak, T. *Collect. Czech. Chem. Commun.* **2001**, *66*, 1149.

(46) Brinkley, D.; Engel, T. *J. Phys. Chem. B* **2000**, *104*, 9836.

(47) Redhead, P. A. *Vacuum* **1962**, *12*, 302.

(48) (a) Henderson, M. A.; Otero-Tapia, S.; Castro, M. E. *Faraday Discuss.* **1999**, *114*, 313. (b) Henderson, M. A. *Langmuir* **1996**, *12*, 5093.
(49) Paul, A.; Bent, B. E. *J. Catal.* **1994**, *147*, 264.
(50) Rodriguez, J. A.; Dvorak, J.; Jirsak, T. *J. Phys. Chem. B* **2000**, *104*, 11515.
(51) Egelhoff, W. F., Jr. *Surf. Sci. Rep.* **1987**, *6*, 253.
(52) Casarin, M.; Maccato, C.; Vittadini, A. *J. Phys. Chem. B* **1998**, *102*, 10745.
(53) Albaret, T.; Finocchi, F.; Noguera, C. *Faraday Discuss.* **1999**, *114*, 285.
(54) Emsley, J. *The Elements*; Clarendon Press: Oxford, 1989; p 180.
(55) Engelking, P. C.; Ellison, G. B.; Lineberger, W. C. *J. Chem. Phys.* **1978**, *69*, 1826.
(56) (a) Rodriguez, J. A.; Hrbek, J.; Kuhn, M.; Chaturvedi, S.; Maiti, A. *J. Chem. Phys.* **2000**, *113*, 11284. (b) Yang, Z.; Wu, R.; Rodriguez, J. A. *Phys. Rev. B* **2002**, *65*, 155409.
(57) Rodriguez, J. A.; Dvorak, J.; Jirsak, T.; Liu, G.; Hrbek, J.; Arai, Y.; Gonzalez, C. *J. Am. Chem. Soc.*, submitted.
(58) Dewar, M. J. S.; McKee, M. L. *J. Comput. Chem.* **1983**, *4*, 84.
(59) (a) Giordano, L.; Goniakowski, J.; Pacchioni, G. *Phys. Rev. B* **2001**, *64*, 075417. (b) Finocchi, F.; Goniakowski, J.; Noguera, C. *Phys. Rev. B* **1999**, *59*, 5178.
(60) (a) Bartkowski, S.; Neumann, M.; Kurmaev, E. Z.; Rubie, D. C. *Phys. Rev. B* **1997**, *56*, 10656. (b) Lindan, P. J. D.; Harrison, N. M.; Gillan, M. J.; White, J. A. *Phys. Rev. B* **1997**, *55*, 15919.